ACI MATERIALS JOURNAL TECHNICAL PAPER

MS No. M-2019-095.R1

Characterization of Iron Ore Tailings as Fine Aggregate

by Sikiru Folahan Oritola, Abdul Latif Saleh, and Abdul Rahman Mohd Sam

Iron ore tailings (IOTs) are common industrial solid waste products which are generated in enormous quantities during the production process of iron ore. By visual observation, this material shows some similarity with natural sand (NS); it was therefore desired to characterize the IOTs to further ascertain their use in concrete. Five types of IOTs obtained from different locations were characterized using microscopic and physical examination techniques. These methods were used to assess the structure and properties of IOTs, subsequently comparing it with that of NS. The surface image of the materials is provided and numerical information, such as the relative concentrations of atoms that comprise the materials, is also indicated. Subsequently, the structure and composition of the IOT materials are identified for possible applications in the construction industry.

Keywords: concrete-making material; fine aggregate; iron ore tailings; microscopy of material; sustainability; waste material.

INTRODUCTION

One of the most important factors for producing workable concrete is the quality of the fine aggregate. Another important factor is good gradation of the aggregates. Due to these basic reasons, it is of paramount significance to study the nature of fine aggregate materials that are used in the production of concrete. Also, in recent time, there has been an increase for construction aggregates all over the world, arising as a result of rapid economic growth of underdeveloped, developing, and developed countries in different regions of the world. Naturally, this growth stimulates the demand for construction materials and on the other hand, there has been increasing amounts of waste generated due to industrial activities in many parts of the world.[1]

The reason for characterizing iron ore tailings (IOTs) is to develop a general classification, which can be attached and related to, according to other researchers and professionals, for the sustainability of the construction industry. The laboratory experimental studies provide the framework for scientific basis and bring to focus the important relationships of sand and IOTs. The particle size distribution gives the fineness modulus number of the material. It also provides the basis of comparing the grading of the material with the British standard (BS) grading limits for fine aggregate. The various density tests describe the relative weight of the IOTs as compared to sand or any other similar material. The porosity also reveals how closely packed the particles of IOTs are in comparison to sand. The X-ray fluorescence indicates the oxides contained in the IOTs. The energy-dispersive X-ray spectroscopy describes the elemental composition of IOTs while the field emission scanning electron microscopy provides the morphology of the material. All the aforementioned properties and microstructure evaluations will aid in categorizing the IOTs as a fine aggregate material for use in concrete.

Some researchers have suggested ways to use tailings in concrete or mortar and some other construction products. The possibility of using graphite ore tailings to partially replace sand in concrete,[2] classification of iron ore fines and suggestion of possible beneficiation,[3] characterization of mine tailings and its usefulness,[4] study of microscopic nature of iron ore,[5] mineralogical classification of iron ore particles,[6] categorization of mortars produced using IOTs as aggregate,[7] use of tailings as aggregates for the production of mortars,[8] and the mineral content and microscopic nature of tailings[9] have been studied and reported. Although some studies have been done in the past with respect to the practicality and application of IOT as construction material, there is still a need for further study of this viable material.

The total accumulation of IOT waste from 2000 to 2009 exceeded 28 billion tons. A large amount of IOTs are stockpiled at various mines all over the world and the current use rate is below 10% of the quantity of IOTs generated as waste from industrial activities.[10] It therefore means that if the waste tailings are consumed in large volume by using them in concrete and mortar production, the problem of finding alternative material for NS would have been solved. Safety is a major concern in civil engineering practice; the possibility of the disposed tailings causing acid mine drainage (AMD) and leaching of heavy metals which harm people and the environment will also be eliminated. Characterizing and thereby establishing means of consuming the tailings will enable the mining industries concerned to meet up with legislation requirements from governmental or other regulating bodies in regard to mine wastes disposal. Cost of tailings dam maintenance will be reduced and loss of soil fertility will also be eliminated. Furthermore, establishing the use of IOTs as a construction product will provide cheaper alternative material for building and civil engineering works and will also ensure economic and environmental sustainability of the iron ore mining industries.

It has also been mentioned that different samples of IOTs may show similar grading but there may be wide variations in the mineral content[11,12]—hence another major reason for conducting this research. To conduct the characterization process, IOTs were sourced from five different locations in Malaysia—namely, Batu Pahat, Muah Jemaluang, Mersing, and two areas in Kota Tinggi. At each location, five samples

ACI Materials Journal, V. 117, No. 2, March 2020.
MS No. M-2019-095.R1, doi: 10.14359/51720305, received March 20, 2019, and reviewed under Institute publication policies.

Table 1—Locations of mines and notations of IOT samples

Notation	Description	Location of mines
ZIOTs	IOTs collected from ZCM, Bhd	Kota Tinggi, Malaysia
LIOTs	IOTs collected from Landas Seketa, Bhd	Kota Tinggi, Malaysia
HIOTs	IOTs collected from Honest Sam, Bhd	Batu Pahat, Cha'ah, Malaysia
GIOTs	IOTs collected from Generasi Karisma, Bhd	Bukit Kampong, Muar, Malaysia
SIOTs	IOTs collected from Sokongan Semulajadi, Bhd	Jamaluang, Mersing, Malaysia

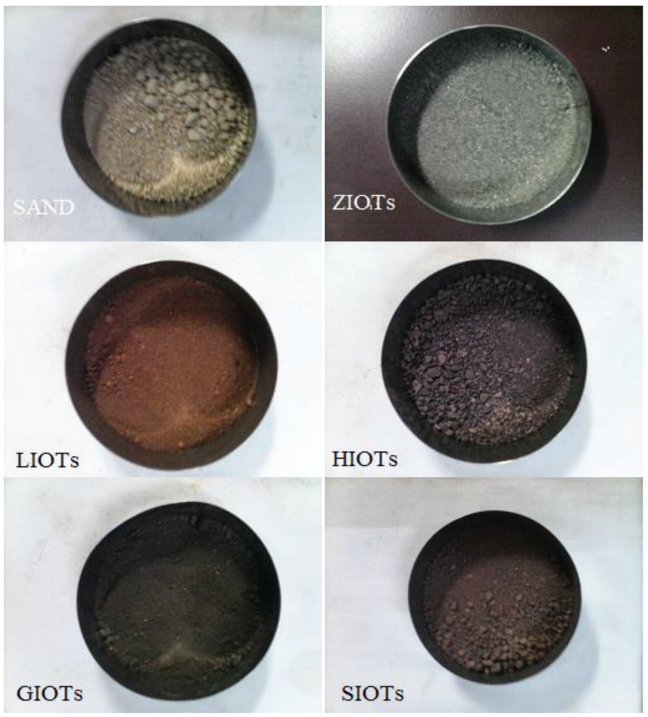

Fig. 1—Images of IOTs compared with NS.

were collected. The average distance between these locations is approximately 200 km. The five types of IOTs obtained from these locations were characterized using qualitative and quantitative techniques.

RESEARCH SIGNIFICANCE

Within the past few years, quite a number of studies have been reported about the use of IOTs in producing concrete. Some even show buildings constructed using IOTs. Most of the studies on this industrial waste product were carried out focusing mainly on its use in concrete. Detailed reports about characterization of IOTs for the purpose of using it in concrete are scarce in technical literature. This present study deals with a detailed study of characterizing IOTs to further establish their use in concrete or mortar and will be very useful in contributing to the advancement of concrete technology.

EXPERIMENTAL PROCEDURE

To characterize the IOTs, the physical properties and the microstructure for the five IOT samples sourced from five different mines and the NS were evaluated. The physical properties determined were particle size distribution, coefficient of uniformity, coefficient of curvature, porosity, specific gravity, fineness modulus, loose unit weight, and compacted unit weight. The chemical and elemental compositions of the materials were also determined. Concrete samples which contain 0% IOTs (control concrete sample) and those with 10, 20, 30, 40, and 50% IOTs replacing sand as fine aggregate were produced. Laboratory experimental tests including density, compressive strength, modulus of elasticity, ultrasonic pulse velocity, water absorption, and sorptivity were conducted on the concrete samples. Also, field emission scanning electron microscopy images of the concrete samples were produced to reveal the morphology of the inner structure of the concrete.

Materials

The materials investigated in this study are five different types of IOTs and NS. The IOTs were sourced from five mines located at different cities. The sources of the IOTs and notations of IOT samples are described in Table 1. The images of the IOTs compared with NS are shown in Fig. 1.

METHODOLOGY

Determination of physical properties of sand and IOTs

The physical properties of sand and IOTs such as particle size distribution were determined in accordance with guidelines specified in BS 812 Part 103.[13] The densities were determined according to specifications in BS EN 1097-3.[14]

X-ray fluorescence and energy dispersive X-ray spectroscopy

The X-ray fluorescence (XRF) was used for chemical analysis to determine the oxide composition of the IOTs, while the elements contained in the IOT samples and those of NS were identified by energy-dispersive X-ray spectroscopy. The guidelines stipulated in the university laboratory manual were followed in carrying out the tests.

Field emission scanning electron microscopy of materials

The microstructure of the NS and IOTs were determined using field emission scanning electron microscopy (FESEM). The NS and IOT material specimens were prepared by making use of an epoxy-impregnated polished section. The epoxy resin was made to permeate the material by encasing with powder particles. Any form of moisture was removed so that it did not interfere with the polymerization of the epoxy. The sand or IOTs specimen, as the case may be, was then placed in a container and surrounded by epoxy, leaving the top surface to be exposed to laboratory

Table 2—Physical properties of IOTs and NS

Physical properties	Aggregates					
	Sand	ZIOT	LIOT	HIOT	GIOT	SIOT
Size passing 600 μm, %	44	95	96	93	97	94
Coefficient of uniformity	3.7	4.7	4.0	3.9	4.1	3.9
Coefficient of curvature	0.02	0.01	0.01	0.01	0.01	0.01
Porosity, %	14	12.1	12.4	11.4	10.4	11.5
Specific gravity	2.65	2.91	2.74	2.79	2.81	2.75
Fineness modulus	3.2	1.4	1.3	1.4	1.1	1.4
Loose unit weight, kg/m^3 (lb/ft^3)	1459 (91.1)	1598 (99.8)	1554 (97.0)	1629 (101.7)	1635 (102.1)	1569 (97.9)
Compacted unit weight, kg/m^3 (lb/ft^3)	1696 (105.9)	1817 (113.4)	1774 (110.7)	1839 (114.8)	1847 (115.3)	1785 (111.4)

air, thereby allowing the low-viscosity epoxy to be drawn into the microstructure by capillary suction.

The morphology of NS and IOTs were characterized using an ultra-high-resolution scanning electron microscope. The fine aggregate materials were placed horizontally at 180 degrees on the substrate holder for surface analysis. The cross-sectional view to observe the thickness was placed at vertical angle of 90 degrees. The microstructure of the samples was then studied at varying magnification.

Determination of properties of hardened concrete for control and IOT concrete samples

The compressive strength of concrete cube samples for the control concrete and those produced using IOTs was determined using a standard uniaxial compression testing machine in the laboratory. Six types of concrete samples were prepared using 0, 10, 20, 30, 40, and 50% replacement level of sand with IOTs. The compressive strength of the cube samples of these concretes was determined at 7, 14, 21, and 28 days. The test was accomplished based on the procedure in BS EN 12390: Part 3.[15] The ultrasonic pulse velocity, density, and modulus of elasticity of concrete samples were also determined following the guidelines in BS EN 12504: Part 4,[16] BS EN 12390: Part 7,[17] and BS EN 12390: Part 13,[18] respectively.

Water absorption and sorptivity test

The water absorption test was done to determine the maximum amount of water that can be absorbed by the control concrete and the IOT concrete samples. It provides a measure of the total, water-permeable pore space in a concrete sample. The water absorption test was conducted according to BS 1881: Part 122.[19]

The sorptivity of the control concrete sample and those containing IOTs as partial replacement for sand was also determined based on guidelines in ASTM C1585-13.[20] The test measures the increase in the mass of a specimen resulting from absorption of water as a function of time.

Determination of FESEM of concrete samples

FESEM was used to evaluate the morphology of the control concrete and those of the IOT concrete samples. The FESEM provides ultra-high-resolution imaging of the concrete samples and describes the details regarding differences that exist in the inner structure of the concrete. The guidelines stipulated in the university laboratory manual were followed in carrying out the test.

EXPERIMENTAL RESULTS AND DISCUSSION

Physical properties of materials

Within the permitted standard limits, the grading of fine aggregate has a greater influence on the properties of concrete than that of coarse aggregate.[21] The particle size distribution of NS and those of the IOTs revealed that the percentage passing the 600 μm sieve was 44% for NS and those of the IOTs varies from 93 to 96%. This indicates availability of finer particles in IOTs compared to the NS. The IOTs recorded specific gravity values ranging from 2.74 to 2.91, while 2.65 was obtained for the NS. The higher the specific gravity of any material, the finer the material.

The fineness modulus of IOTs ranges from 1.1 to 1.4 while that of NS was 3.2. For fine aggregate materials, if the value of the fineness modulus is lower in comparison to another, this suggests that the material with the lower value is finer.[21] The test result values for the specific gravity, the percentage passing the 600 μm sieve, and the fineness modulus indicate a similar trend, thereby ratifying the availability of more fines particles in IOTs compared with the NS. The physical properties of the IOTs and NS are shown in Table 2. The particle size distribution of ZIOTs, LIOTs, HIOTs, GIOTs, SIOTs and those of NS are graphically compared in Fig. 2, which also indicate the British Standard (BS) grading limits for fine aggregate materials.

Oxide composition in IOTs

The major oxides in the IOT sample ZIOTs, as compared to those available in Nigeria, China, and India,[11] are indicated in Fig. 3. The figure revealed that the dominant oxide in IOT sample ZIOTs and the other locations mentioned is silicon dioxide (SiO_2). From Fig. 3, it can be seen that the oxide composition of ZIOTs can be compared with IOTs from other sources. It can also be deduced that the common oxides in IOTs with high percentages are silicon dioxide, iron oxide, and aluminum oxide.

Energy-dispersive X-ray spectroscopy

The elements contained in all the IOT samples and those of NS as identified by energy-dispersive X-ray spectros-

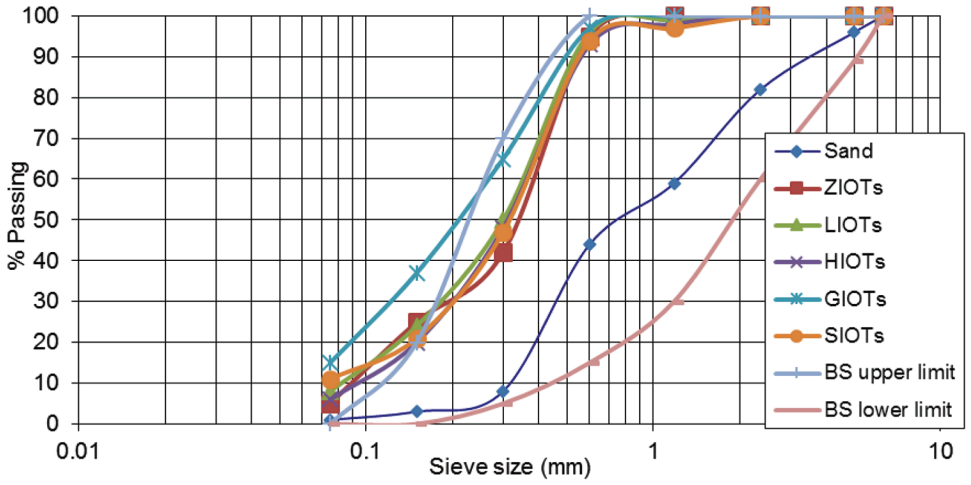

Fig. 2—Particle size distribution of IOTs and NS.

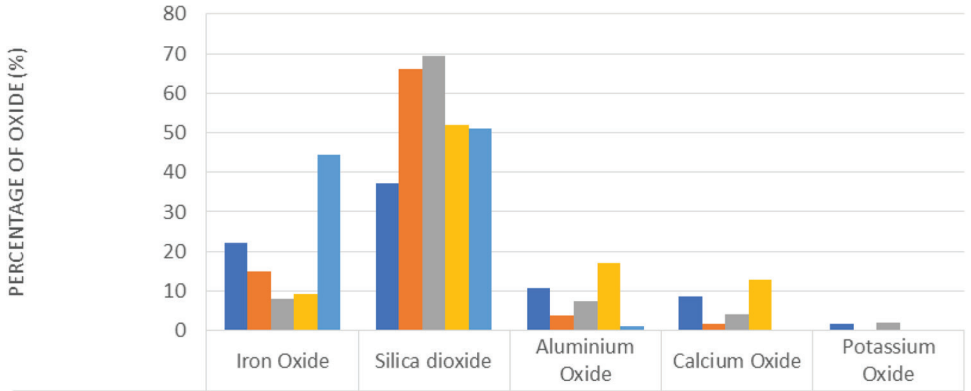

	Iron Oxide	Silica dioxide	Aluminium Oxide	Calcium Oxide	Potassium Oxide
K. Tinggi Malaysia	22.1	37.2	10.7	8.5	1.7
Itakpe Nigeria	15	66	3.8	1.8	0
Miyun China	8.1	69.5	7.4	4.1	2
Sujing China	9.1	52.1	17.1	12.7	0.3
Goa India	44.4	51.1	1.2	0.2	0

Fig. 3—Major oxides contained in IOTs.

Table 3—Composition of chemical elements in IOTs and NS

Chemical elements	Percentage by weight composition, %					
	NS	ZIOTs	LIOTs	HIOTs	GIOTs	SIOTs
Oxygen	49.0	33.4	32.2	30.0	31.4	31.7
Silicon	27.4	20.0	19.5	20.6	18.5	21.8
Iron	—	19.3	15.7	16.4	15.6	19.7
Aluminum	12.3	5,5	5.9	6.4	8.2	9.8
Carbon	6.4	12.6	18.1	16.7	17.7	8.7
Fluorine	—	5.3	4.5	5.7	4.7	4.3
Titanium	0.1	0.2	0.2	0.1	0.1	0.3
Moisture	4.7	3.5	3.7	4.1	3.6	3.5

copy are summarized in Table 3. Figures 4 and 5 show the energy levels of each X-ray photon present in the elements contained in NS and ZIOTs, respectively. The energy of each X-ray photon is characteristic of the element which produced it. The dominant elements in the IOT samples as revealed by the energy-dispersive X-ray spectroscopy results are silicon, iron, and aluminum. This result shows some similarities with the outcome of the X-ray fluorescence, which indicates the dominance of silicon dioxide, iron oxide, and aluminum oxide in the IOTs.

Morphology of IOTs and NS

The field emission scanning electron microscopy (FESEM) provides the morphology of IOTs and those of the NS. The

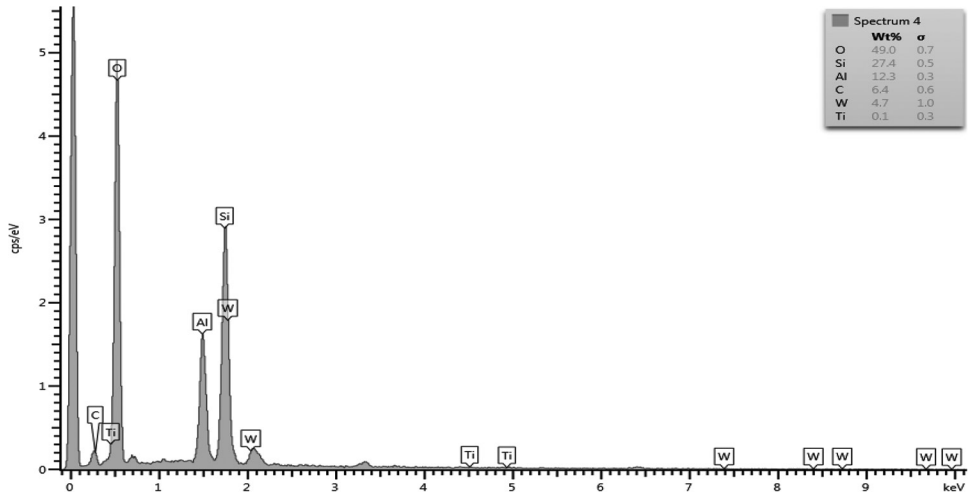

Fig. 4—Energy-dispersive spectroscopy of NS.

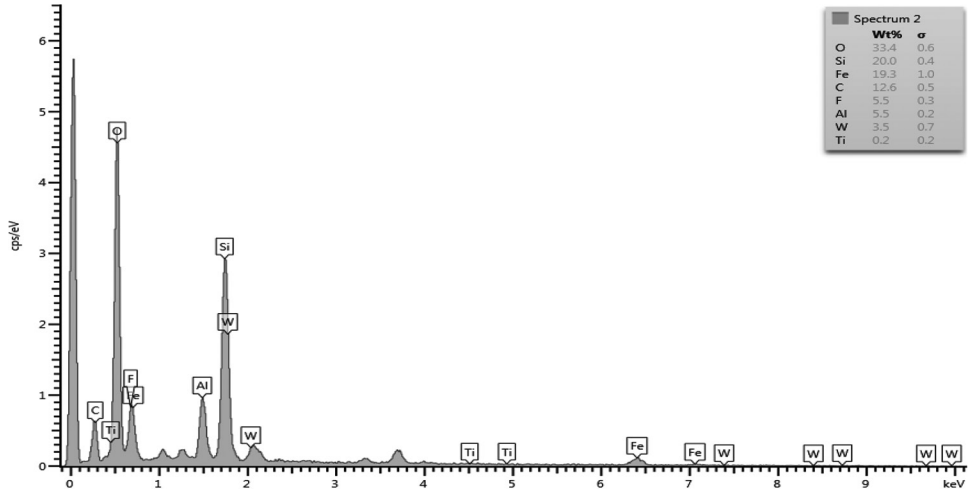

Fig. 5—Energy-dispersive spectroscopy of ZIOTs.

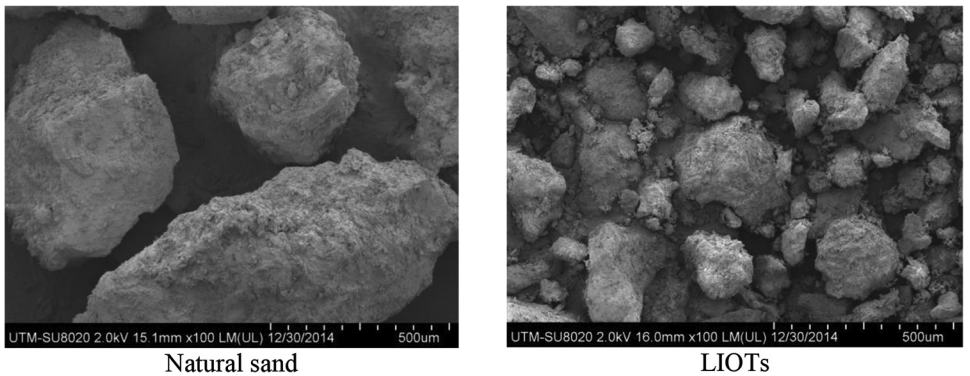

Natural sand LIOTs

Fig. 6—FESEM morphology of NS versus LIOTs at 500 µm magnification.

morphology of the NS at varying magnifications scale in contrast to those of IOTs are shown in Fig. 6 through 9. The FESEM morphology reveals that, using the same magnifications, more grain particles of IOTs are observed compared with the NS within the same area of coverage. This suggests that the particles of the IOTs are more densely packed in contrast to the NS. In any event, if these two materials were to be used for production of mortar or concrete, it is likely that more grain particles of the IOTs may be more available for combination with the cement paste, compared to the NS.

Properties of hardened concrete for control and IOTs concrete

The compressive strength is the most important representative index for concrete because concrete is used in a structure to resist mainly compression force, and other properties of concrete can be related to the compressive strength. The compressive strength test results for the control concrete and those produced using IOTs from ZCM at 10, 20, 30, 40, and 50% replacement level of sand are shown in Fig. 10. On completion of 28 days of curing in water, the concrete

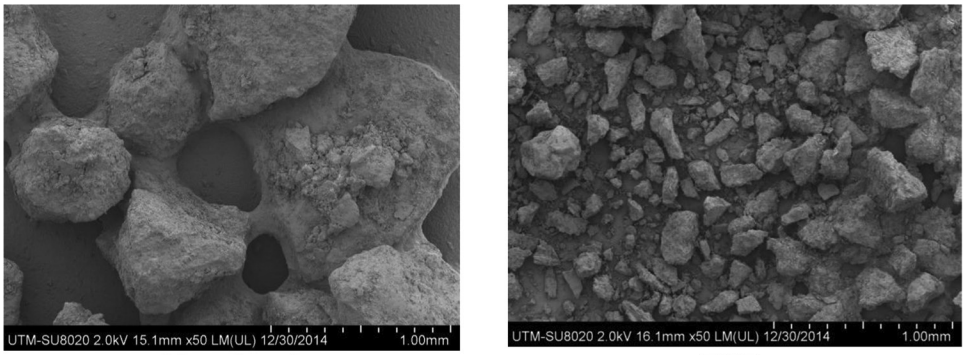

Fig. 7—FESEM morphology of NS versus ZIOTs at 1 mm magnification.

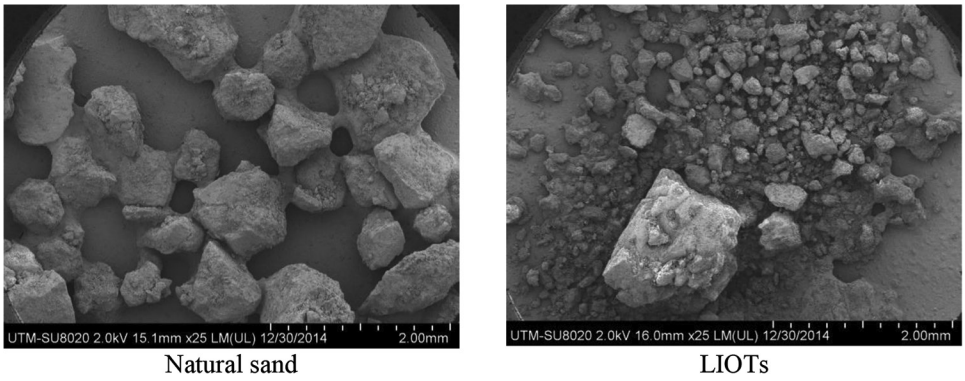

Fig. 8—FESEM morphology of NS versus LIOTs at 2 mm magnification.

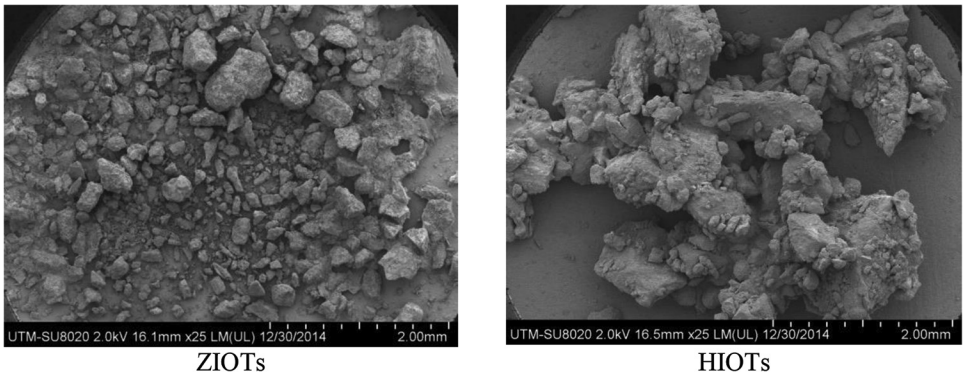

Fig. 9—FESEM morphology of ZIOTs and HIOTs at 2 mm magnification.

sample CZT30 recorded the highest compressive strength of 43.7 N/mm^2, while the smallest value of 35.4 N/mm^2 was recorded by the control concrete sample CT0. The IOT concrete CZT30 recorded 23.4% higher value in compressive strength than the control concrete. The texture of the IOTs is rough and angular, and this could be responsible for the increase in strength of the concrete samples containing IOTs in varying percentage. For the same water-cement ratio (*w*/*c*) and cement content, the compressive strength of the concrete mixture is mainly influenced by the composition of the granular skeleton.[21] The density, modulus of elasticity, and ultrasonic pulse velocity test results for the control concrete and those containing IOTs that was collected from ZCM are depicted in Table 4. The concrete containing IOTs recorded 3.6% higher value in density than the control concrete, indicating that the IOTs concrete is denser than the control concrete. The modulus of elasticity of concrete is affected by the modulus of elasticity of the aggregate and by their volumetric proportion in the concrete.[21] Under the same stress, stronger concrete exhibits a lower strain. This implies that high-strength concrete has a higher modulus of elasticity. Experimental results from this study show that the modulus of elasticity increases with increase in the compressive strength of the concrete samples tested. The modulus of elasticity of the concrete samples is an indicator property and serves as basis for further comparison of the concrete properties. The IOTs concrete sample CZT30 recorded the highest elastic modulus value of 28.1 GPa, which is 19.6% more than the value recorded by the control concrete. If the value of pulse velocity of any concrete is greater than 4.5 km/s, the quality of the concrete is considered to be excellent and if the value fall below 3.0 km/s, the quality of the concrete is doubtful. Experimental results for all the samples tested falls within the range of 3.5 to 4.5 km/s, which

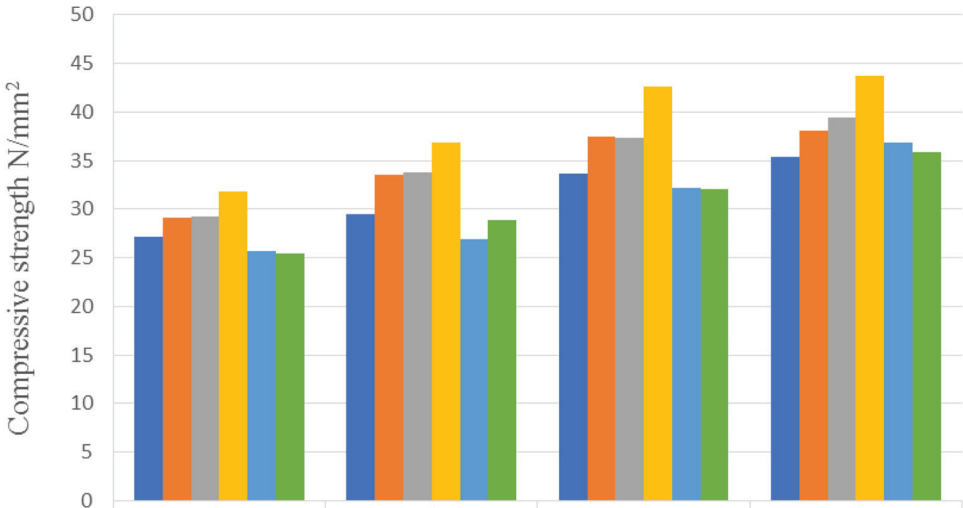

	7 days	14 days	21 days	28 days
CT0	27.2	29.5	33.7	35.4
CZT10	29.1	33.5	37.5	38.1
CZT20	29.3	33.8	37.3	39.4
CZT30	31.8	36.9	42.6	43.7
CZT40	25.7	26.9	32.2	36.8
CZT50	25.5	28.9	32.1	35.9

Fig. 10—Compressive strength of control and IOT concrete.

Table 4—Density, modulus of elasticity, and ultrasonic pulse velocity of control and IOT concrete

Concrete sample	Description of concrete sample	Density, kg/m (lb/ft^3)	Modulus of elasticity, GPa (psi)	UPV, km/s (m/s)
CT0	Control concrete sample—0% IOTs content in fine aggregate	2350 (146.7)	23.5 (3408)	4.35 (2.70)
CZT10	Concrete sample—10% IOTs content in fine aggregate	2390 (149.2)	24.9 (3611)	4.36 (2.71)
CZT20	Concrete sample—20% IOTs content in fine aggregate	2395 (149.5)	25.5 (3698)	4.37 (2.72)
CZT30	Concrete sample—30% IOTs content in fine aggregate	2430 (151.7)	28.1 (4076)	4.39 (2.73)
CZT40	Concrete sample—40% IOTs content in fine aggregate	2435 (152.0)	24.3 (3524)	4.41 (2.74)
CZT50	Concrete sample—50% IOTs content in fine aggregate	2435 (152.0)	23.1 (3350)	4.43 (2.75)

is considered good. The IOTs concrete CZT50 recorded a higher percentage increase of 1.8% over the control concrete, indicating that the IOTs concrete is denser in structure.

Water absorption and sorptivity of control and IOT concrete samples

The water absorption test results provide a measure of the total water-permeable pore space in the concrete samples. Experimental results show that the concrete samples containing IOTs performed better than the control sample in terms of water resistance. The water absorption test results gave indication regarding the effectiveness of the IOTs and being able to reduce the permeable pore space in the concrete. To further buttress this point, the correlation between the water absorption and ultrasonic pulse velocity of concrete samples is indicated in Fig. 11. It can be observed that there is a strong, inversely proportional relationship between water absorption and ultrasonic pulse velocity of IOT concrete. These results suggest that the small particle size of IOTs was able to fill the pore space in concrete, thereby producing more dense concrete, which gave higher values of ultrasonic pulse velocity and reduced water absorption.

The sorptivity test results gave the rate of absorption of water by capillary suction of unsaturated concrete, which was placed in contact with water. The results gave an indication of the quality of the outer zone of concrete members, which can be very useful when dealing with concrete cover to reinforcement. The outcome of this experimental study revealed that increasing the content of IOTs as fine aggregate in concrete results in lower values of sorptivity, implying that the rate of absorption of water by capillary suction of unsaturated concrete decreases with the addition of IOTs. The correlation that exists between the sorptivity of IOT concrete with the ultrasonic pulse velocity is similar to that displayed by the water absorption behavior. The relationship between sorptivity and ultrasonic pulse velocity of control concrete and the IOT concrete samples is shown in Fig. 12.

FESEM morphology of concrete

The FESEM shows the difference in morphology of concrete samples containing IOTs compared with the control

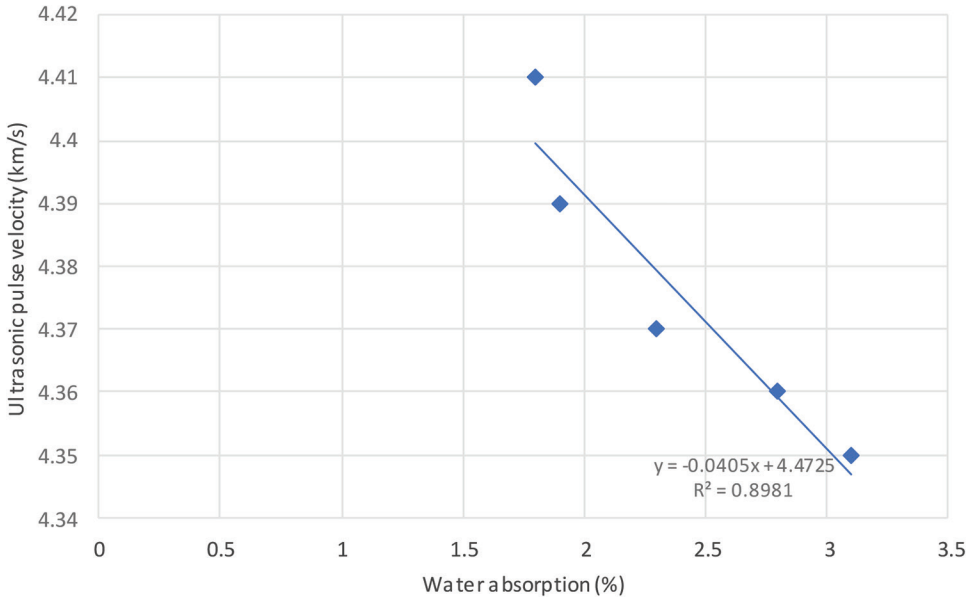

Fig. 11—Relationship between water absorption and ultrasonic pulse velocity of control and IOT concrete.

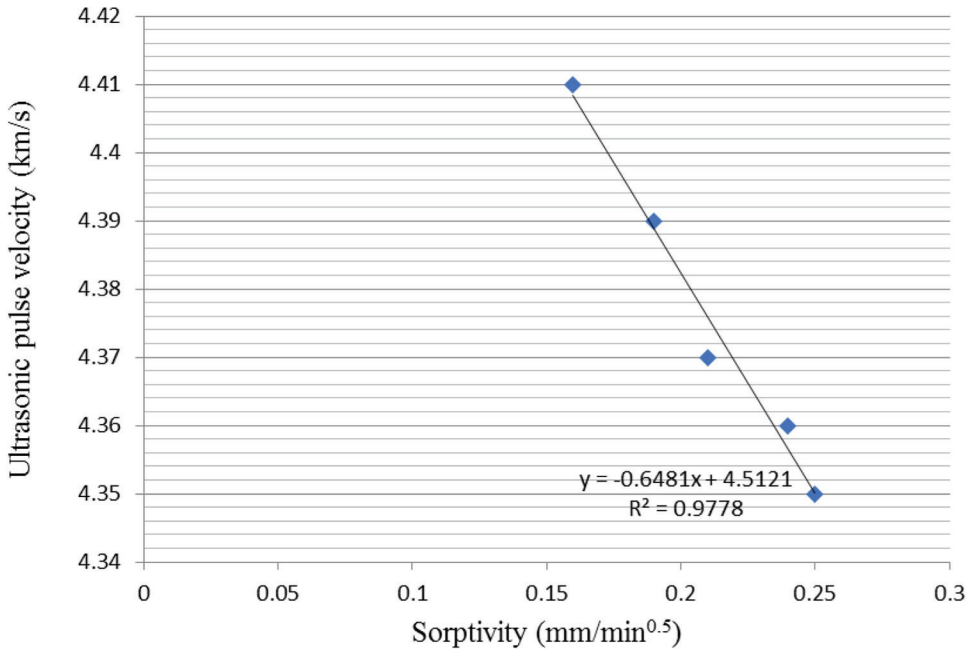

Fig. 12—Relationship between sorptivity and ultrasonic pulse velocity of IOT concrete.

sample. The FESEM morphology of the control concrete sample at magnification scale of 500 nm in comparison to that of the IOT concrete is shown in Fig. 13. At magnification of 500 nm, the images show the hexagonal shape, which is common to indicate the presence of calcium hydroxide (CaOH); the needle-like shape, which normally reveals ettringite; and sheet-like shape of calcium-silicate-hydrate (C-S-H) exhibited by the concrete samples. The FESEM image of the control concrete sample shows a crystal grow into a void where space restrictions are minimal. In the case of the IOT concrete, the pattern revealed by the FESEM image shows a crystal form in which the sheet-like shape and fine bundles commonly displayed by calcium-silicate-hydrate (C-S-H) and the ettringite needles can be seen. The existence of the distinctive morphologies depends on the availability of void space for uninhibited growth in the concrete.

CONCLUSIONS

Based on the results of experimental investigation conducted under laboratory conditions, the following deductions with regards to characterization of IOTs are drawn:

1. Due to tighter particle surface depicted by IOTs, it suggests that the material may be more effective in reducing the pore space in concrete, thereby improving the compactness of concrete.

2. The use of IOTs as fine aggregate can find applications in the industry, where it is desired to have highly dense concrete. It can also aid in improving the water resistance of concrete and the dimensional stability.

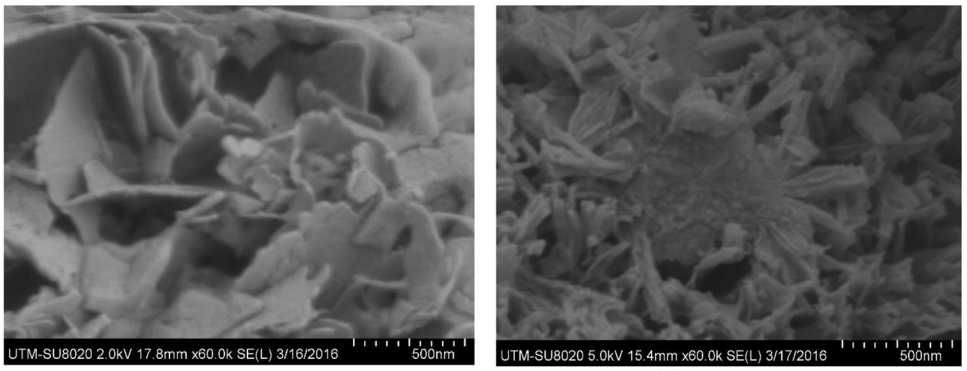

control concrete IOTs concrete

Fig. 13—FESEM morphology of control concrete sample versus IOT concrete at 500 nm.

3. The chemical composition of the IOTs as revealed by the X-ray fluorescence results indicates the dominance of silicon dioxide, iron oxide, and aluminum oxide in the material. This suggests that IOTs can be used as supplementary material to improve the strength of concrete.

4. Characterization of IOTs before using it as fine aggregate is strongly suggested for the purpose of knowing the physical properties, chemical content, and morphology of the material. This will assist the concrete mixture designer in choosing the best type of material to use.

5. The characterization of the IOTs will lead to the development of general classifications, which can be attached and related to, by other researchers and professionals, for the sustainability of the construction industry

AUTHOR BIOS

ACI member **Sikiru Folahan Oritola** *is a Lecturer 1 at Federal University of Technology, Minna, Nigeria, where he received his BS and MS. He received his PhD from Universiti Teknologi Malaysia, Skudai, Malaysia. His research interests include use of waste material in concrete structures.*

Abdul Latif Saleh *is a Professor in the Faculty of Civil Engineering at Universiti Teknologi Malaysia. His research interests include concrete and structural analysis of reinforced concrete structures.*

Abdul Rahman Mohd Sam *is an Associate Professor in the Faculty of Civil Engineering at Universiti Teknologi Malaysia. His research interests include ceramics and polymer in concrete.*

ACKNOWLEDGMENTS

This research was sponsored by RUG, Universiti Teknologi Malaysia with research grant Number Q.J130000.2505.09H37. The authors are grateful for the contributions of N. Huda, Mr. Hasibul, and Mr. Abdulrahman for collection of iron ore tailings samples at the iron ore mines. We also express our gratitude and sincere appreciation for the support of all technical staff for their assistance in the laboratory.

REFERENCES

1. Jorge, B., and Rui, S., "Use of Waste Materials in the Production of Concrete," *Key Engineering Materials*, V. 634, 2015, pp. 85-96.

2. Kathirvel, P.; Kwon, S. J.; Lee, H. S.; Karthick, S.; and Saraswathy, V., "Graphite Ore Tailings as Partial Replacement of Sand in Concrete," *ACI Materials Journal*, V. 115, No. 3, May 2018, pp. 481-492.

3. Patra, S.; Pattanaik, A.; and Rayasam, V., "Characterisation of Low-Grade Barsua Iron Ore Fines and Identification of Possible Beneficiation Strategies," *Canadian Metallurgical Quarterly*, V. 58, No. 1, 2019, pp. 28-45. doi: 10.1080/00084433.2018.1516598

4. Ceniceros-Gómez, A. E.; Macías-Macías, K. Y.; Cruz-Moreno, J. E.; Gutiérrez-Ruiz, M. E.; and Martínez-Jardines, L. G., "Characterization of Mining Tailings in México for the Possible Recovery of Strategic Elements," *Journal of South American Earth Sciences*, V. 88, 2018, pp. 72-79. doi: 10.1016/j.jsames.2018.08.013

5. Donskoi, E.; Manuel, J. R.; Austin, P.; Peterson, M. J.; and Hapugoda, S., "Comparative Study of Iron Ore Characterisation Using a Scanning Electron Microscope and Optical Image Analysis," *Transactions of the Institution of Mining and Metallurgy Section B. Applied Earth Science*, V. 122, No. 4, 2014, pp. 217-229. doi: 10.1179/1743275814Y.0000000042

6. He, J.; Liu, C.; Hong, P.; Luo, Z.; and Zhao, L., "Mineralogical Characterization of the Typical Coarse Iron Ore Particles and the Potential to Discharge Waste Gangue Using a Dry Density-Based Gravity Separation," *Powder Technology*, V. 342, 2019, pp. 348-355. doi: 10.1016/j.powtec.2018.10.010

7. Carrasco, E. V. M.; Magalhaes, M. D. C.; Santos, W. J. D.; Alves, R. C.; and Mantilla, J. N. R., "Characterization of Mortars with Iron Ore Tailings Using Destructive and Nondestructive Tests," *Construction and Building Materials*, V. 131, 2017, pp. 31-38. doi: 10.1016/j.conbuildmat.2016.11.065

8. Argane, R.; Benzaazoua, M.; Hakkou, R.; and Bouamrane, A., "Reuse of Base-Metal Tailings as Aggregates for Rendering Mortars: Assessment of Immobilization Performances and Environmental Behavior," *Construction and Building Materials*, V. 96, 2015, pp. 296-306. doi: 10.1016/j.conbuildmat.2015.08.029

9. Zanko, L. M.; Niles, H. B.; and Oreskovich, J. A., "Mineralogical and Microscopic Evaluation of Coarse Taconite Tailings from Minnesota Taconite Operations," *Regulatory Toxicology and Pharmacology*, V. 52, No. 1, 2008, pp. 51-65. doi: 10.1016/j.yrtph.2007.09.016

10. Huang, X.; Li, V. C.; and Ranade, R., "Feasibility Study of Developing Green ECC Using Iron Ore Tailings Powder as Cement Replacement," *Journal of Materials in Civil Engineering*, ASCE, V. 25, No. 7, 2013, pp. 923-931. doi: 10.1061/(ASCE)MT.1943-5533.0000674

11. Oritola, S. F.; Saleh, A. L.; and Mohd Sam, A. R., "Performance of Iron Ore Tailings as Partial Replacement for Sand in Concrete," *Applied Mechanics and Materials*, V. 735, 2015, pp. 122-127.

12. Saleh, A. L.; Mohd Sam, A. R.; Zakaria, R.; Mushairry, M.; and Oritola, S. F., "Effect of Iron ore Tailings on the Drying Shrinkage of Concrete," The 11th International Civil Engineering Post Graduate Conference – The 1st International Symposium on Expertise of Engineering Design SEPKA-ISEED 2016, UTM, Johor, Malaysia, pp. 20-34.

13. BS 812: Part 103, "Methods for Determination of Particle Size Distribution," British Standards Institution, London, UK, 1985.

14. BS EN: 1097-3, "Testing Aggregates Part 2: Methods for Determination of Density," British Standards Institution, London, UK, 1998.

15. BS EN 12390: Part 3, "Method for Determination of Compressive Strength of Concrete Cubes," British Standards Institution, London, UK, 2009.

16. BS EN 12504: Part 4, "Method for Determination of Ultrasonic Pulse Velocity of Concrete," British Standards Institution, London, UK, 2004.

17. BS EN 12390: Part 7, "Method for Determination of Hardened Density of Concrete," British Standards Institution, London, UK, 2009.

18. BS EN 12390-13, "Testing Hardened Concrete. Determination of Secant Modulus of Elasticity in Compression," British Standards Institution, London, UK, 2013.

19. BS 1881: Part 122, "Method for Determination of Water Absorption of Concrete," British Standards Institution, London, UK, 2011.

20. ASTM C1585-13, "Standard Test Method for Measurement of Rate of Absorption of Water by Hydraulic Cement Concretes," ASTM International, West Conshohocken, PA, 2013, 6 pp.

21. Neville, A. M., *Properties of Concrete*, John Wiley & Sons, Inc., London, UK, 2011.